Domain and Segment Orientation Behavior of PBS–PTMG Segmented Block Copolymers

HAN SUP LEE,[1] HAE DONG PARK,[1] CHANG KI CHO[2]

[1] Department of Textile Engineering, Inha University, 253 Younghyun-Dong, Nam-Ku, Inchon, 402-751, Korea
[2] Department of Textile Engineering, Hanyang University, 17 Haengdang-Dong, Seongdang-Ku, Seoul, 133-791, Korea

Received 2 October 1999; accepted 10 December 1999

ABSTRACT: Segment and domain orientation behaviors of a series of poly(butylene succinate) (PBS) –poly(tetramethylene glycol) (PTMG) segmented block copolymers containing different amounts of hard segment were studied with synchrotron small-angle X-ray scattering (SAXS) and infrared dichroic methods. Copolymers used in this work consist of PBS as a hard segment, and poly(tetramethylene oxide) (PTMO) of molecular weight 2000g/mol as a soft segment. As hard-segment content increased, phase-separated morphology changed from a phase of continuous soft matrix containing isolated hard domain to one of continuous hard matrix. Upon stretching, domains responded differently depending on their initial orientation. Based on SAXS results, two major domain deformation modes, that is, lamellar separation and shear compression, were suggested. The orientation behavior of the hard and soft segments was examined with infrared dichroic method. Upon drawing, the orientation function of the crystalline hard segment decreased at low-draw ratios. It was interpreted in terms of rotation of long axis of hard domain along the stretching direction. The lowest value of the orientation function of PBS30 was approximately −0.5, that is, theoretical minimum. This result seems to indicate that for PBS30 containing about 30% hard segment, rotation of hard domain occurs without appreciable interdomain interaction, which is consistent with the morphological model suggested on the basis of SAXS results. Plastic deformation of the hard domain due to domain breakup was found to occur at low-draw ratios for the sample containing higher hard-segment content. Domain mechanical stability was tested by drawing a sample up to three different maximum draw ratios.
 J Appl Polym Sci 77: 699–709, 2000

Key words: domain and segmental orientation; segmented block copolymer; SAXS; infrared dichroism; uniaxial drawing

INTRODUCTION

A polymer chain in thermoplastic elastomers consists of two chemically-distinct segments usually called hard and soft segments. Because of repulsive interaction between two constituent segments, they undergo microphase-separation process, resulting in phase-separated heterogeneous structure of hard and soft domains.[1,2] Hard domains are usually glassy or crystalline at room temperature and act as physical crosslinking sites, whereas soft domains are rubbery, rendering long-range elasticity.

Many physical properties of thermoplastic elastomers such as elasticity, toughness, and initial modulus can be understood by analyzing morphological changes of phase-separated domain structure during deformation process. Structural

Correspondence to: H. S. Lee (hslee@dragon.inha.ac.kr).
Contract grant sponsor: 1999 INHA University Research Program, MOST, and POSCO, Korea.

Journal of Applied Polymer Science, Vol. 77, 699–709 (2000)

changes occurring during the deformation process range from microscopic segmental orientation to macroscopic domain deformation. Therefore, to establish the structure–property relationship of thermoplastic elastomers, structural changes occurring during a deformation process have to be carefully investigated at various levels. A number of instrumental methods were successfully applied to analyze the orientation and deformation behavior of thermoplastic elastomers. Especially, infrared dichroism[3–7] and small-angle X-ray scattering (SAXS)[8–10] method were frequently used to access the segmental orientation and domain deformation behavior.

It has been well established with an infrared dichroic method that two segments in thermoplastic elastomers behave quite differently during uniaxial deformation process.[3–7] Even though the orientation function of soft segment increases continuously with drawing, that of the hard segment might decrease during the early stage of the deformation process. The decreased orientation function was generally interpreted in terms of the rotation of the long axis of two-dimensional lamellar plane along the deformation direction. Upon further drawing, hard domains might undergo plastic deformation, resulting in the orientation of individual hard segment, not hard domain, along the stretching direction. SAXS study on the domain orientation and deformation behavior might provide conclusive evidence to correctly interpret the experimental results on segmental orientation behavior.

SAXS method was shown to be quite useful to characterize the macroscopic domain restructuring process.[11–13] From studies on the deformation of oriented polyethylene, Pope and Keller[14] suggested four different types of deformation processes: lamellar slip, chain slip, lamellar separation, and fibrillar slip. On the basis of SAXS results on three different polyurethanes under tensile strain, Desper et al.[15] suggested three possible deformation modes: shear mode, tensile mode, and rotation or transition of independent particles. Each mode was found to be mainly operational with a particular type of polyurethane. It was also mentioned that deformation mode of a particular polymer might be influenced by details of chemical composition and morphology.

Pakula et al. studied morphological changes related to deformation of styrene–butadiene–styrene triblock block copolymers with a cylindrical microdomain structure using SAXS method.[16] From the scattering profiles observed at low deformations, they found that several structural changes such as yielding, fragmentation, and reorientation of the domains might occur. The detailed nature and the sequences of these processes were strongly dependent on the orientation of the domains to the stretching direction. However, the structural state reached at high deformation was almost the same for all samples, with which a four-point scattering pattern was observed with the scattering lobes of intensity maxima elongated along the direction perpendicular to the stretching. A four-point scattering pattern was also observed from the deformation studies of segmented poly(urethaneurea) by Shibayama et al.[17] It was also interpreted in terms of the rotation of the domains in the spherulite texture.

In this study, structural changes occurring during uniaxial deformation and relaxation of PBS–PTMG segmented block copolymers were investigated with an infrared dichroism and synchrotron SAXS methods. The effect of hard-segment content on the phase-separated morphology was also characterized. By combining experimental observations obtained at two different levels, mechanical properties of PBS–PTMG copolymers were correlated with the internal physical structure.

EXPERIMENTAL

Samples

Initially, one mole of succinic acid (Shinyo Chemical, Japan) was reacted with two moles of 1,4-butanediol (Junsei Chemical, Japan) to form bis(hydroxybutyl succinate) (BHBS). PBS–PTMG segmented block copolymer was then synthesized by reacting BHBS with an appropriate mole of PTMG (M_n: 2000 g/mol). Chemical structure of PBS–PTMG copolymer is shown in Figure 1. Details of the synthesizing condition and method can be found elsewhere.[18] The hard-segment content in each PBS–PTMG copolymer was measured with 200 MHz ^{1}H-NMR and shown in Table I. Sample names in Table I indicate the type of hard segment and weight percent of hard segment. Molecular weights and polydispersity of each sample are also shown in the table.

PBS–PTMG copolymers were initially dissolved in chloroform solvent and cast onto a glass plate. After evaporating most solvent at room temperature, film was further dried in a vacuum

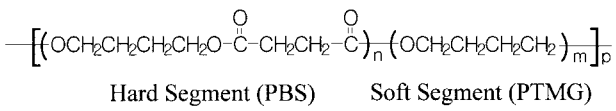

Figure 1 Chemical structure of PBS–PTMG segmented block copolymer.

oven overnight. PBS30 was annealed at 60°C and others at 70°C for 12 h.

SAXS Measurements

SAXS experiments were conducted at the beam line 3C2, PAL (Pohang Accelerator Laboratory), Korea. Details about the beam line have been described elsewhere.[19,20] Monochromatic light was obtained with a Si (111) double-crystal monochromator. A one-dimensional diode-array detector was used. Samples (approximately 10 × 30 × 1 mm) were deformed uniaxially with a mechanical stretcher built in this laboratory. During uniaxial extension, the sample width was allowed to contract. The stretcher could be rotated around beam path to obtain scattering patterns at various directions. The sample was relaxed at a given draw ratio for about 5 min before SAXS pattern was obtained. Five minutes of relaxation time were observed to be enough to allow the pseudo-equilibrium state at the given draw ratio. To obtain the scattering only from the sample, routine corrections such as sample attenuation, parasitic and background scattering, and incident intensity fluctuation were performed. Scattering vector q in this work is defined as

$$q = \frac{4\pi}{\lambda} \sin \theta \tag{1}$$

where 2θ is the scattering angle and λ is a wavelength of 1.608 Å. Domain repeat distance (d-spacing, d) was obtained from the scattering vector at maximum intensity ($q_{\max}$):

$$d = \frac{2\pi}{q_{\max}} \tag{2}$$

Infrared Dichroism

Infrared spectra were obtained with a Nicolet Model 520 Fourier transform infrared spectrometer. Spectral resolution was maintained at 2 cm^{-1}. Polarization of the incident infrared radiation was achieved with an aluminum wire polarizer on a KRS-5 substrate. Two infrared spectra were collected successively with a polarizer parallel and perpendicular to the stretching direction. From two absorbances ($A_{\parallel}$, $A_{\perp}$) obtained from a particular infrared band in two corresponding spectra (parallel, perpendicular), dichroic ratio (D) was calculated

$$D = \frac{A_{\parallel}}{A_{\perp}} \tag{3}$$

Orientation function (f) was obtained with the following relationship:

$$f = \frac{D_0 + 2}{D_0 - 1}\frac{D - 1}{D + 2} \tag{4}$$

D_0 is the dichroic ratio of a corresponding peak in a perfectly oriented state and defined as

$$D_0 = 2 \cot^2 \alpha \tag{5}$$

where α is an angle between the transition dipole moment of a corresponding infrared band and polymer chain direction.

Differential Scanning Calorimetry (DSC)

DSC thermograms were obtained with a Shimadzu DSC-50. Heating rate was 10°C/min and sample mass for each experiment was about 10 mg.

RESULTS AND DISCUSSION

Domain Orientation and Deformation

In Figure 2, the d-spacing is plotted as a function of hard-segment content in PBS–PTMG segmented block copolymers. With an increase of hard-segment content up to approximately 50%, d-spacing decreased. Further increase of the

Table I HS Content, Average Molecular Weight, and Polydisperse Index for PBS–PTMG Copolymers Used in This Work

Sample	HS Content (wt %)	$\bar{M}_n$ (g/mol)	$\bar{M}_w$ (g/mol)	$\bar{M}_n/\bar{M}_w$
PBS30	29.8	32,600	59,600	1.83
PBS45	43.2	17,000	92,000	5.41
PBS55	52.7	49,100	122,400	2.49

HS, hard segment.

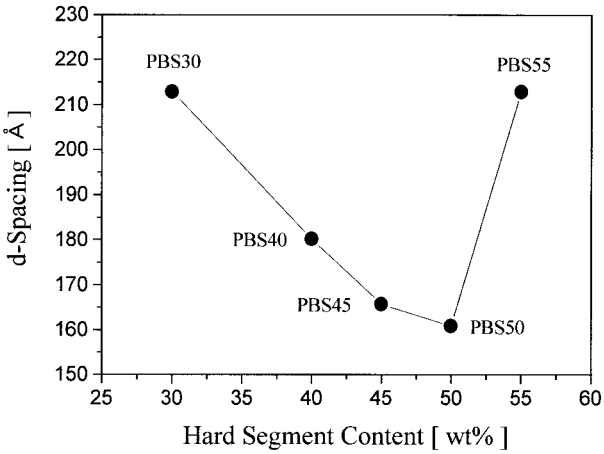

Figure 2 *d*-Spacing change as a function of HS content.

hard-segment content caused an abrupt increase of *d*-spacing. This type of behavior is very different from the corresponding one obtained with the polyurethane having rigid hard segment.[21,22] Li et al.[23] investigated the effect of hard-segment flexibility on the multiphase structure of segmented polyurethanes. Polyurethanes, which were expected to have extended hard-segment conformation owing to low flexibility of hard segments, showed increased *d*-spacing with the increase of hard-segment content. However, *d*-spacing of polyurethanes with flexible hard segment was found to be insensitive to the increasing hard-segment content. Hard domains in PBS–PTMG consist of mainly PBS, in which all atoms along a main chain are connected with flexible single covalent bonds. However, the hard segments in PBS–PTMG were found to crystallize at room temperature, resulting in rigid hard domain. Because PBS homopolymer was found to crystallize into lamellae, the hard domain of PBS–PTMS is expected to form a two-dimensional lamellar-type structure.[24,25] The difference between results in Figure 2 and those by Li et al. might be attributed to the different hard-domain structure.

The results in Figure 2 may be interpreted with the schematic model shown in Figure 3. If the hard-segment content is well below 50%, hard domains are expected to exist as isolated domains in a continuous soft-domain matrix [Fig. 3(a)]. By increasing the hard-segment content, the number of hard domains in an unit volume will increase, resulting in decreased repeat distance between the hard domains, as shown in Figure 2. However, samples with a hard-segment content above 50% are believed to have different morphology [Fig. 3(c)]. Isolated soft domains are believed to be dispersed in a continuous hard-domain matrix. Further increase of hard-segment content with samples of the type shown in Figure 3(c) will show increased repeat distance between soft domains.

The schematic model in Figure 3 suggests that phase inversion from a continuous soft domain to a continuous hard domain might occur at around 50% hard-segment content. Phase inversion will be accompanied by significant changes of mechanical properties. If external stress is applied to the structure of microphase-separated morphology with soft-domain continuous phase [Fig. 3 (a)], most of initial deformation will occur at the rubbery soft-domain matrix. Upon phase inversion, semicrystalline hard domains have to undergo initial deformation. In Figure 4, initial moduli obtained from stress–strain curves of all samples used in this work are plotted with the hard-segment content. Initial modulus stays almost constant with the increasing hard-segment content,

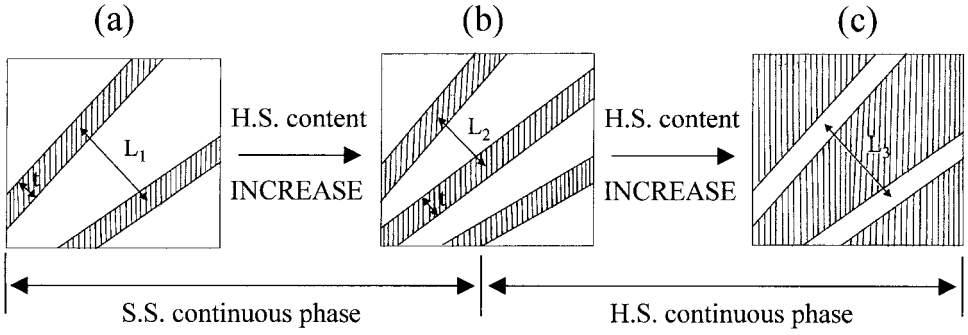

Figure 3 Schematic models of phase-separated PBS–PTMG copolymers having different hard-segment HS content.

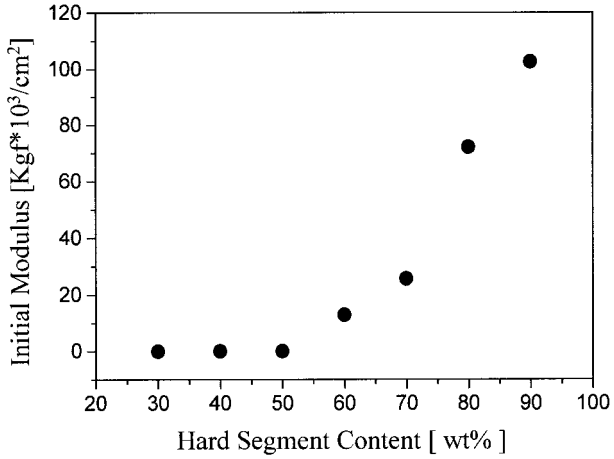

Figure 4 Initial modulus change as a function of HS content.

whereas hard-segment content remains below 50%. Upon further increase of the hard-segment content above 50%, abrupt increase of the initial modulus was observed, as expected. The phase-inversion phenomenon was also studied with polyurethanes by Chang et al.[26] Based on transmission electron microscopy and initial modulus results, phase inversion was confirmed to occur at approximately 50% hard-segment content.

Before drawing, orientation of hard domains should be randomly distributed, resulting in macroscopically isotropic state. If external stress is applied, each domain will respond differently, depending on the relative domain orientation with respect to the stretching direction. To facilitate the interpretation of SAXS profiles obtained during the uniaxial deformation process, the deformation models for two characteristic domains are

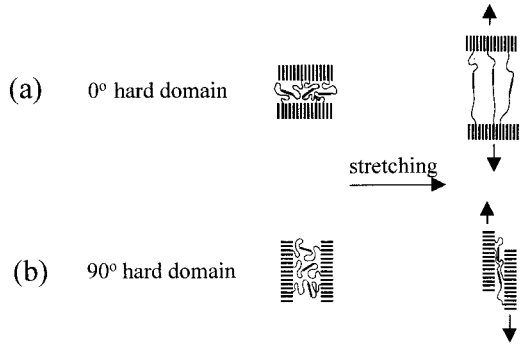

Figure 5 Schematic model for the deformation of two domains oriented parallel (0° hard domain) and perpendicular (90° hard domain) to the stretching direction (stretching direction is vertical).

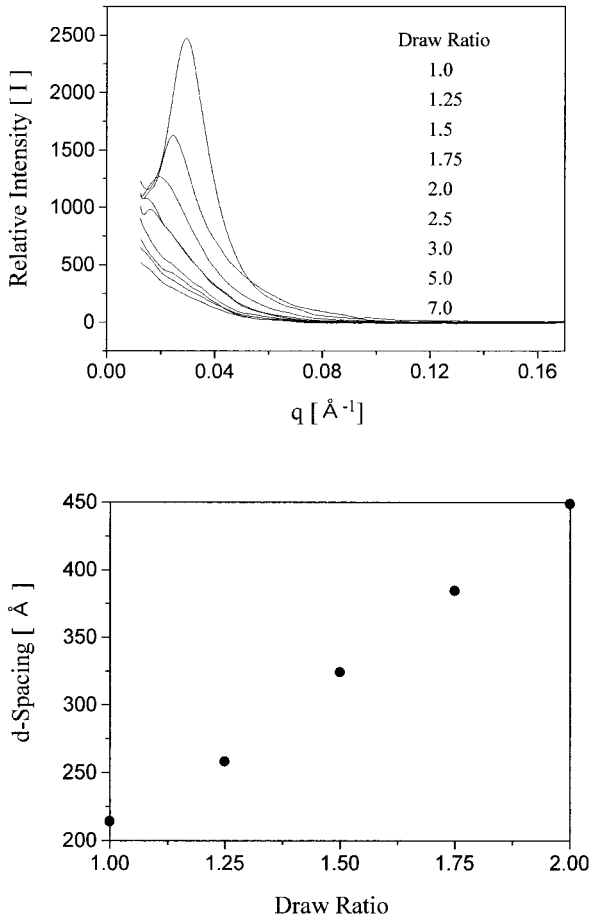

Figure 6 SAXS profiles (meridional scan) (top) and *d*-spacing (bottom) of PBS30.

considered (Fig. 5). Domains of which domain axes (perpendicular to the hard-domain plane) are parallel/perpendicular to the stretching direction will be called 0° hard domain/90° hard domain, as shown in Figure 5(a,b). Upon deformation at low-draw ratios, soft segments between two adjacent 0° hard domains will be extended along the stretching direction, causing the increase of *d*-spacing [Fig. 5(a)]. This type of deformation was called lamellar separation by Pope and Keller[14] and as tensile mode by Desper et al.[15] Deformation mode of 90° hard domains will be shear compression. Because the soft segments residing in 90° hard domains [Fig. 5(b)] are also expected to be oriented along the stretching direction, *d*-spacing between 90° hard domains will be decreased.

In Figure 6(a), SAXS profiles of PBS30 sample obtained with one-dimensional position-sensitive detector parallel to the stretching direction are shown (meridional scan). Scattering intensity

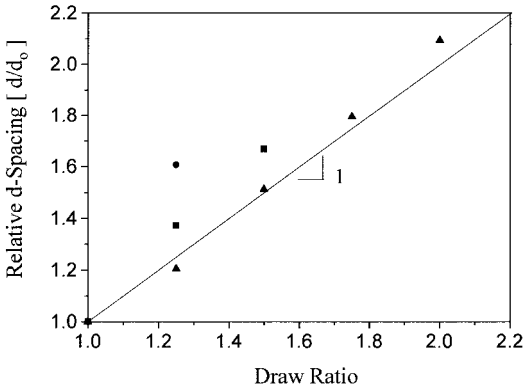

Figure 7 Relative *d*-spacing obtained from meridional scan as a function of draw ratio: (▲) PBS30, (■) PBS45, (●) PBS55.

along this direction is contributed mainly by 0° hard domains [Fig. 5(a)]. Therefore, the deformation behavior of that domain can be inferred from the scattering profiles in Figure 6(a). It is obvious that the scattering maximum decreases continuously with draw ratio, as expected from the model in Figure 5(a). The decreased scattering intensity is due to the internal structural change as well as decreased scattering volume. Note that the effect of decreased sample thickness during stretching is not corrected in Figure 6(a). The *d*-spacing obtained from the scattering vector with maximum intensity is also plotted in Figure 6(b). The *d*-spacing appears to increase almost linearly with the draw ratio.

Relative domain spacing (d/d_0; *d*-spacing at each draw ratio divided by that before drawing) obtained from the meridional scan are shown in Figure 7. A straight line with a slope of one is also shown. It is clear that for PBS30 the initial deformation behavior of 0° hard domains is very close to affine deformation: the macroscopic change of sample length along the stretching direction is linearly proportional to the microscopic *d*-spacing change along the corresponding direction. The size of hard domains in PBS30 appears to be small enough to secure affine deformation with tensile mode without significant interaction between domain stack. Similar observations have been reported from many studies,[27] including a study by Fakirov et al.,[28] who studied PBT–PEG thermoplastic elastomers. However, the deformation behavior of samples containing higher hard-segment content seems to deviate from affine behavior. As the hard-segment content increases as in PBS45, domain size becomes large enough to show appreciable interaction between domain stacks. As mentioned in Figure 3, PBS55 sample seems to have a hard domain as a continuous matrix. Significant deviation from affine deformation as shown in Figure 7 with PBS55 might be attributed to the phase inversion occurring at approximately 50% hard-segment content.

Similar interpretation was suggested by Desper et al.[15] based on the SAXS studies with two different types of polyurethanes. Deformation in tensile mode (similar to lamellar separation by Pope and Keller[14]) was preferentially observed with the diol-cured polyurethane which has hard-segment particles responding like cylinders in which the thickness and diameter are comparable. In contrast, amine-cured polyurethane, which has good structural integrity owing to stronger interaction between hard segment, tends to deform through shear mode.

SAXS profiles obtained with one-dimensional detector direction perpendicular to the stretching direction are shown in Figure 8(a) (equatorial

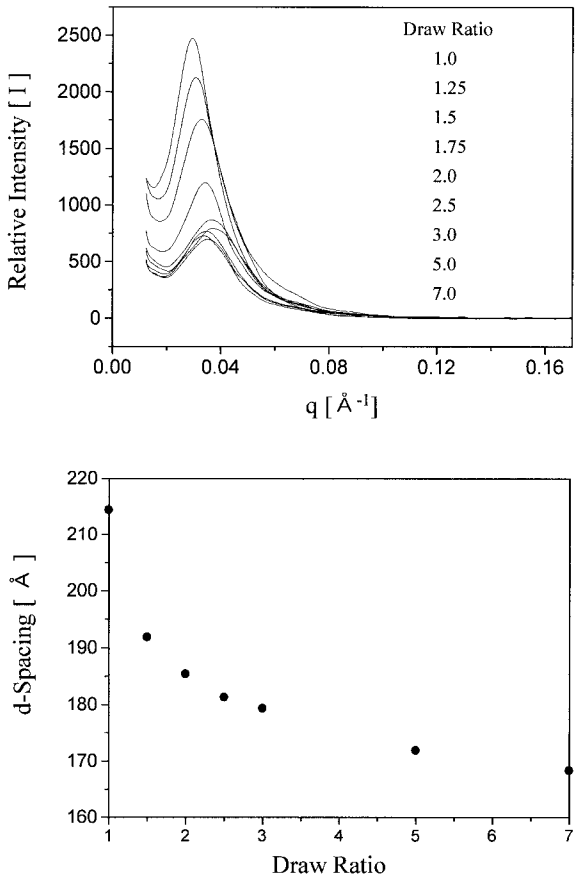

Figure 8 SAXS profiles (equatorial scan) (top) and *d*-spacing (bottom) of PBS30.

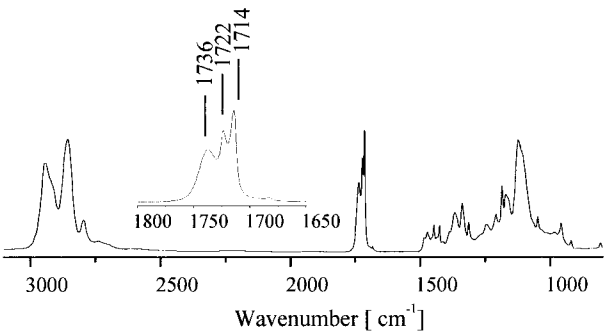

Figure 9 IR spectrum of PBS 30.

scan). Contrary to the profiles in the meridional scan, the position of the intensity maximum shifts continuously with increasing draw ratio, indicating a decreasing *d*-spacing with the draw ratio, as shown in Figure 8(b). Note that the scattering intensity in Figure 8(a) is contributed mainly by the 90° hard domain. This result is consistent with the deformation model shown in Figure 5(b). This type of deformation mode corresponds to lamellar slip by Pope and Keller.[14]

The deformation behavior of many domains inclined to the stretching direction can be understood with a combination of two deformation modes shown in Figure 5. Exact contribution of each deformation mode will be dependent on the inclination angle of a domain with respect to the stretching direction. The deformation modes in Figure 5 are believed to be mainly operative at low-draw ratios. Mechanical integrity of hard domain cannot be preserved at high-raw ratio. If domain breakup starts to happen at high-raw ratio, structural change will be much more complex to understand just with one characterizing method. Results on the mechanical stability of the hard domains will be discussed later.

Segmental Orientation

Even though SAXS method is conveniently applied to elucidate the deformation behavior at the macroscopic domain level, infrared dichroism method can provide further insight on the deformation behavior at the localized segmental level. With the infrared dichroism method, the orientation behavior of hard and soft segment can be monitored selectively. In Figure 9, overall infrared spectrum of PBS45 is shown. Band assignment for the bands used in this work are shown in Table II. Note that the carbonyl stretching band between 1750–1700 cm^{-1} is split into three bands

Table II Assignment of Infrared Bands for PBS–PTMG Copolymer Used in this Work

Wavenumbers (cm^{-1})	Assignment	A/C[a]
1736	C═O stretching, SS	A
1722	C═O stretching, HS	C
1714	C═O stretching, HS	C
1110	C—O stretching, SS	A

[a]A, amorphous; C, crystal; SS, soft segment; HS, hard segment.

centered at 1736, 1722, and 1714 cm^{-1}. As the hard-segment content increased in PBS–PTMG copolymer, intensities of bands at 1714 and 1722 cm^{-1} increased, whereas that at 1736 cm^{-1} decreased. To further verify the assignment of three carbonyl-stretching bands in Table II, infrared spectra were collected while a sample was being heated up to the melting temperature of hard domain. It was found that with the increasing temperature absorbance of band at 1736 cm^{-1} increased at the expense of that of two bands at 1714 and 1722 cm^{-1}. Upon melting, carbonyl-stretching band consisted of single band at about 1736 cm^{-1}. From these results, it can be concluded that those bands at 1714 and 1722 cm^{-1} are related to the crystalline hard segment and at 1736 cm^{-1} to the hard segments in amorphous state.

In Figure 10, relative peak area (absorbance of bands at 1714 and 1722 cm^{-1} divided by absorbance of total carbonyl stretching band) is plotted as a function of crystallinity of hard segment ob-

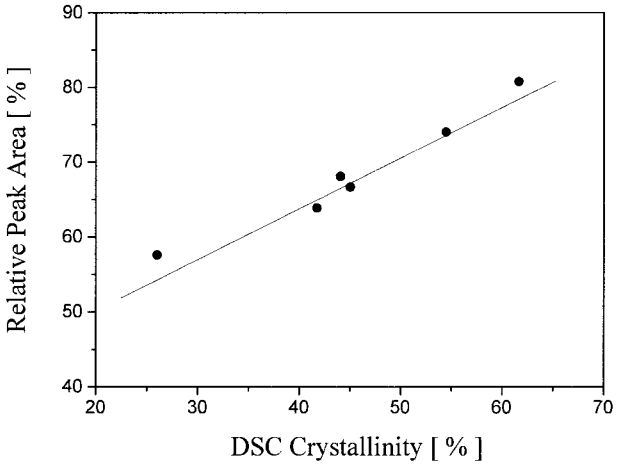

Figure 10 Relative peak area of two crystalline C═O stretching bands versus DSC crystallinity.

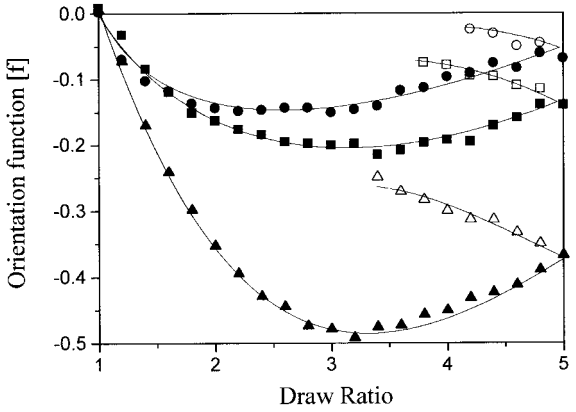

Figure 11 Orientation function of a band at 1714 cm^{-1} as a function of draw ratio obtained during extension: (▲) PBS30, (■) PBS 45, (●) PBS55, and during relaxation: (△) PBS30, (□) PBS 45, (○) PBS55.

tained with DSC thermograms of all samples used. Crystallinity was calculated from enthalpy change of fusion of a particular sample divided by that of ideal PBS crystal.[29] Once again, the linear relationship between the relative band absorbance and the crystallinity indicates that two carbonyl-stretching bands at 1714 and 1722 cm^{-1} can be assigned to the hard segment in a crystalline state. Therefore, orientation of crystalline hard segment can be inferred from the orientation behavior of those two crystalline carbonyl-stretching bands.

Three samples were uniaxially deformed up to draw ratio 5 and relaxed down to the point until the tensile stress became negligible. Assuming $\alpha = 78°$,[7] the orientation function of band at 1714 cm^{-1} during a cycle of deformation process was calculated for three samples and are shown in Figure 11. As the draw ratio increases, the orientation function of this band for three samples decreases initially and reaches a minimum point before it starts to increase. Negative orientation values suggest that upon extension, the long axis (parallel to hard-domain plane) of hard domains, not hard segment, tends to orient along the stretching direction, resulting in orientation of the hard segment inside the crystalline hard domain along the direction perpendicular to the stretching direction. This type of deformation behavior was reported in a number of studies for the orientation of hard segments in two-dimensional lamellar domains.[3,5] The negative orientation function value in Figure 11 indicates that the crystalline hard domains maintain its mechanical integrity during the initial deformation process.

One striking aspect of Figure 11 is that the minimum orientation function value of PBS30 reaches about −0.5, which is the theoretical minimum for a segment oriented perfectly perpendicular to the stretching direction. Based on SAXS results, it was suggested that hard domains in PBS30 exist as isolated islands in continuous soft-segment matrix. Because there is no significant interdomain interaction during initial deformation period, stretching of this sample may apply strong shear force to most hard domains inclined to the stretching direction and thus rotate the crystalline hard domains to form 0° hard domains.

Even though the orientation function change of this band in three samples shows qualitatively similar behavior, quantitative orientation value is markedly different. Minimum orientation functions of PBS45 and PBS55 are not as low as that of PBS30. Although the orientation function of PBS30 reaches minimum at about draw ratio 3.25, that of PBS45 and PBS55 becomes minimum at draw ratios of approximately 2.75 and 2.25, respectively. These results indicate, as suggested from SAXS results, that for PBS45 and PBS55, there is increased interdomain interaction during stretching process, causing hard-domain breakup at relatively lower draw ratios. It is to be noted that the orientation function value obtained during the extension process is quite different from that during the relaxation process. This fact also suggests plastic hard-domain breakup occurred during the stretching process.

Soft-segment orientation behavior was examined from the orientation function change of C—O stretching band at 1110 cm^{-1}. Even though there is a small contribution of the hard segment to the absorbance of this band, absorbance of C—O stretching band at 1100 cm^{-1} is mainly due to ether functional groups in soft segments. Therefore, orientation behavior of the soft segment can be accessed from the dichroic behavior of C—O stretching band with minor experimental error. Assuming $\alpha = 0°$, the orientation function of C—O stretching peak of three samples is calculated and plotted in Figure 12 as a function of draw ratio. As expected, the orientation function at draw ratio zero is negligible, confirming an isotropic structure before drawing. The orientation function of this band increases continuously with an increasing draw ratio and decreases during the relaxation period. Contrary to the results in Figure 11, orientation function during the extension period is always higher than the corre-

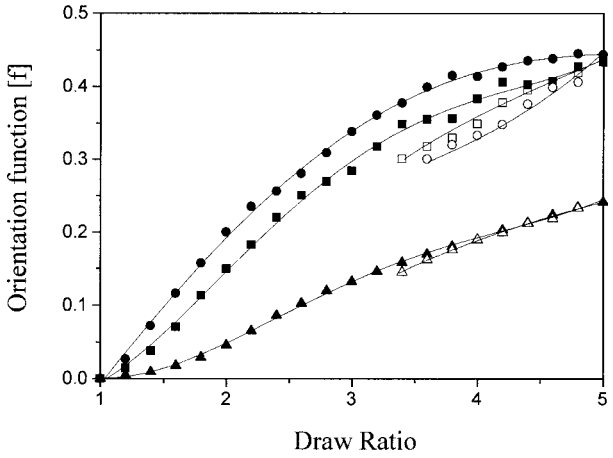

Figure 12 Orientation of function of a band at 1110 cm^{-1} as a function of draw ratio obtained during extension: (▲) PBS30, (■) PBS 45, (●) PBS55, and during relaxation: (△) PBS30, (□) PBS 45, (○) PBS55.

sponding value during the relaxation period. Because the glass transition of soft segment is well below room temperature, soft segment in extended conformation tends to recoil back to relaxed conformation owing to the entropic restoring force.[30]

It can be easily noted from Figure 12 that the orientation function during the extension period increases with hard-segment content. Because PBS30 sample has continuous soft-segment matrix, orientation of soft segment can relax easily. However, orientation relaxation of the soft segment in PBS55 will be retarded by the continuous hard domain. This result is consistent with the results in Figures 2 and 3. Careful examination of Figure 12 will reveal that hysteresis, difference between the orientation function during extension and that during relaxation period, of PBS30 sample is appreciably smaller than those of PBS45 and PBS55. It was mentioned with Figure 11 that, compared with other two samples, upturn of orientation function of crystalline carbonyl-stretching band of PBS30 was observed at higher draw ratio. Because major plastic deformation owing to hard-domain breakup was expected to start at that upturning point of orientation function of the crystalline carbonyl-stretching band, the amount of plastic deformation in PBS30 during the extension period would be smaller. Lower hysteresis in the soft-segment orientation of PBS30 in Figure 12 is consistent with the results obtained from the hard-segment orientation behavior.

Domain Mechanical Stability

To test hard-domain breakup phenomenon in more detail, PBS45 samples were stretched up to three different maximum draw ratios and relaxed. Orientation functions of three carbonyl-stretching bands obtained during a cycle of deformation are shown in Figure 13. If stress is removed after it was stretched up to maximum draw ratio 2, the sample returned almost completely to the original state. Furthermore, there is no appreciable hysteresis in the orientation functions of all three carbonyl bands [Fig. 13(a)]. However, a small amount of hysteresis can be observed for the sample stretched up to draw ratio 3 [Fig. 13(b)]. If the sample is stretched up to draw ratio 5, which is well above the draw ratio at which plastic domain deformation starts to occur, significant hysteresis can be found [Fig. 13(c)]. Based on the results in this figure, it can be concluded that hard domains of PBS45 are deformed elastically as long as draw ratio remains below approximately 3. Upon further drawing beyond draw ratio 3, domain breakup starts to occur, resulting in plastic deformation of the hard domains. It is interesting to note that carbonyl band at 1736 cm^{-1} which was assigned to the hard segment dispersed in the soft domain shows almost complete elastic behavior during the entire range of draw ratio studied in this work. This fact, once again, supports the band assignment of three carbonyl-stretching peaks in Table II.

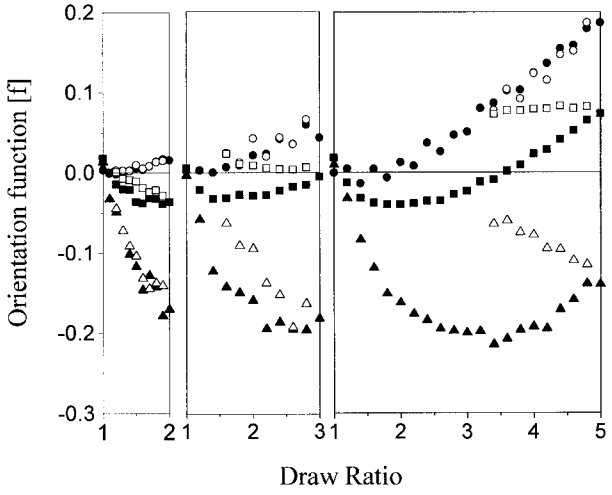

Figure 13 Orientation functions of three C═O stretching bands of PBS 45 samples drawn up to three different maximum draw ratios obtained during extension: (▲) 1736 cm^{-1}, (■) 1722 cm^{-1}, (●) 1714 cm^{-1}, and during relaxation: (△) 1736 cm^{-1}, (□) 1722 cm^{-1}, (○) 1714 cm^{-1}.

CONCLUSION

Domain and segmental deformation behaviors of a series of PBS–PTMG segmented block copolymers containing different amounts of hard segment were studied with synchrotron SAXS and FTIR dichroism methods. Based on the change in *d*-spacing and initial modulus as a function of hard-segment content, morphology of PBS–PTMG segmented block copolymer was suggested. As hard-segment content increased, the morphology was found to change from a phase of continuous soft-domain matrix containing isolated hard domains to one of continuous hard-domain matrix with dispersed soft domains, as shown schematically in Figure 2. This type of phase inversion appears to occur at approximately 50% hard-segment content.

Upon stretching, hard domains responded differently depending upon their initial orientation. In the case of 0° hard domains, initial deformation was an extension of the soft segment between two adjacent hard domains along the stretching direction, resulting in increased *d*-spacing. If hard-segment content was low enough to have isolated hard domains in a continuous soft matrix, increase of the *d*-spacing was found to be affine. As hard-segment content increased to about 43%, deformation in lamellar separation mode starts to deviate from affine behavior. Initial deformation of 90° hard domains could be interpreted with shear compression or lamellar slip. Both deformation modes were believed to be operative for the deformation of domains inclined to the stretching direction.

Segmental orientation behavior was analyzed with infrared dichroic method. The orientation of the crystalline hard segment was obtained from the orientation function of carbonyl stretching band at 1714 cm^{-1}. As draw ratio increased, orientation function decreased initially until it reached minimum value. The decreasing orientation function with draw ratio was interpreted in terms of the orientation of long axis of hard domains along the stretching direction. Minimum orientation function value of PBS30 was close to -0.5, which is theoretical minimum. This fact suggested that the rotation of most hard domains inclined to the stretching direction was almost perfect for PBS30 sample, in which hard domains could be aligned without significant interdomain interaction. Even though there was an appreciable hysteresis during a cycle of hard-segment deformation, the deformation of soft segment was observed to be quite elastic.

Mechanical integrity of hard domains during deformation process was also examined by stretching one sample (PBS45) to three different maximum draw ratios. If stretched up to draw ratio 2, all three carbonyl-stretching bands showed completely elastic behavior. However, samples drawn to draw ratio 5 showed significant plastic deformation behavior for the two crystalline carbonyl-stretching bands. From this result, it was concluded that domain breakup started to occur at the draw ratio corresponding to the minimum orientation value of crystalline carbonyl-stretching band.

This work was supported by the 1999 INHA University Research Program. The X-ray experiments at PLS, Korea, were supported by MOST and POSCO, Korea.

REFERENCES

1. Goodman, I. Developments in Block Copolymers; Applied Science: London, New York, 1985; Chapter 6.
2. Mark, N. M.; Bikales, C. G. Encyclopedia of Polymer Science and Engineering, 2nd ed.; Wiley: New York, 1988; vol. 12, 75–117.
3. Lee, H. S.; Lee, N. W.; Paik, K. H.; Ihm, D. W. Macromolecules 1994, 27, 4364–4370.
4. Jasse, B.; Koenig, J. L. J Macromol Sci Rev Macromol Chem 1979, C17(1), 61–135.
5. Wang, C. B.; Cooper, S. L. Macromolecules 1983, 16, 775–786.
6. Reynolds, N.; Spiess, H. W. Macromol Chem Phys 1994, 195, 2855–2873.
7. Estes, G. M.; Seymour, R. W.; Cooper, S. L. Macromolecules 1971, 4, 452–457.
8. Gerasimov, V. I.; Genin, Y. V.; Tsvankin, D. Y. J Polym Sci: Polym Phys Ed 1974, 12, 2035–2046.
9. Goschel, U. Polymer 1995, 36, 1157–1165.
10. Stribeck, N.; Fakirov, S.; Sapoundjieva, D. Macromolecules 1999, 32, 3368–3378.
11. Young, P.; Stein, R. S.; Kyu, T. J Polym Sci, Part B: Polym Phys 1990 28, 1791–1812.
12. Stribeck, N.; Sapoundjieva, D.; Denchev, Z.; Apostolov, A. A.; Zachmann, H. G.; Stamm, M.; Fakirov, S. Macromolecules 1997, 30, 1329–1339.
13. Murthy, N. S.; Bednarczyk, C.; Moore, R. A. F.; Grubb, D. T. J Polym Sci, Part B: Polym Phys 1996, 34, 821–835.
14. Pope, D. P.; Keller, A. J Polym Sci: Polym Phys Ed 1975, 13, 533–566.
15. Desper, C. R.; Schneider, N. S.; Jasinski, J. P. Macromolecules 1985, 18, 2755–2761.

16. Pakula, T.; Saijo, K.; Kawai, H.; Hashimoto, T. Macromolecules 1985, 18, 1294–1302.
17. Shibayama, M.; Ohki, Y.; Kotani, T.; Nomura, S. Polymer J 1987, 19, 1067–1080.
18. Park, Y. H.; Cho, C. G. Polymer (Korea) 1998, 22, 559–569.
19. Pohang Accelerator Laboratory, Web Page, http://palweb.postech.ac.kr/.
20. Park, B. J.; Rah, S. Y.; Park, Y. J.; Lee, K. B.; Rev Sci Instrum 1995, 66, 1722–1724.
21. Abouzahr, S.; Wilkes, G. L.; Ophir, Z. Polymer 1982, 23, 1077–1087.
22. Koberstein, J. T.; Galambos, A. F.; Leung, L. M. Macromolecules 1992, 25, 6195–6204.
23. Li, Y.; Ren, Z.; Zhao, M.; Yang, H.; Chu, B. Macromolecules 1993, 26, 612–622.
24. Kanamoto, T. J Polym Sci: Polym Phys Ed 1974, 12, 2535–2549.
25. Ihn, K. J.; Yoo, E. S.; Im, S. S. Macromolecules 1995, 28, 2460–2464.
26. Chang, A. L.; Briber, R. M.; Thomas, E. L.; Zdrahala, R. J.; Critchfield, F. E. Polymer 1982, 23, 1060–1068.
27. Prasman, E.; Thomas, E. L. J Polym Sci, Part B: Polym Phys 1998, 36, 1625–1636.
28. Fakirov, S.; Fakirov, C.; Fischer, E. W.; Stamm, M.; Apostolov, A. A. Colloid Polym Sci 1993, 271, 811–823.
29. Miyata, T.; Masuko, T. Polymer 1998, 39, 1399–1404.
30. Young, R. J.; Lovell, P. A. Introduction to Polymers, 2nd ed.; Chapman & Hall: London, 1991, Chapter 3.